

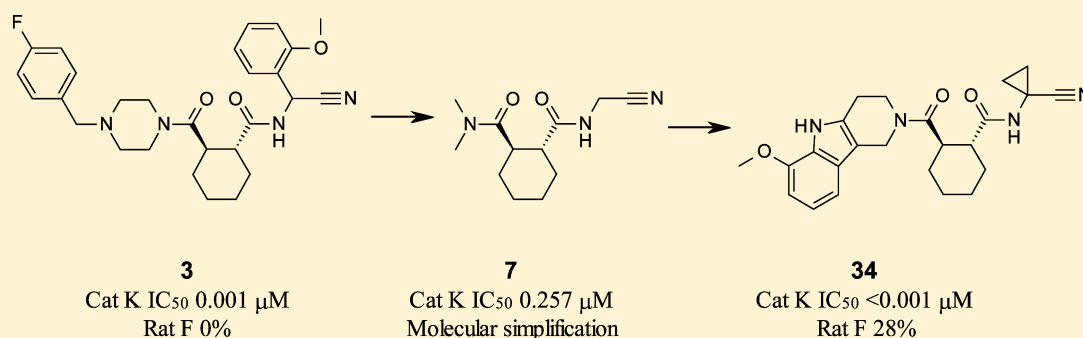
# (1*R*,2*R*)-*N*-(1-Cyanocyclopropyl)-2-(6-methoxy-1,3,4,5-tetrahydropyrido[4,3-*b*]indole-2-carbonyl)cyclohexanecarboxamide (AZD4996): A Potent and Highly Selective Cathepsin K Inhibitor for the Treatment of Osteoarthritis

Alexander G. Dossetter,<sup>\*,†</sup> Howard Beeley,<sup>†</sup> Jonathan Bowyer,<sup>†</sup> Calum R. Cook,<sup>†</sup> James J. Crawford,<sup>†</sup> Jonathan E. Finlayson,<sup>†</sup> Nicola M. Heron,<sup>†</sup> Christine Heyes,<sup>†</sup> Adrian J. Highton,<sup>†</sup> Julian A. Hudson,<sup>†</sup> Anja Jestel,<sup>‡</sup> Peter W. Kenny,<sup>†</sup> Stephan Krapp,<sup>‡</sup> Scott Martin,<sup>†</sup> Philip A. MacFaul,<sup>†</sup> Thomas M. McGuire,<sup>†</sup> Pablo Morentin Gutierrez,<sup>†</sup> Andrew D. Morley,<sup>†</sup> Jeffrey J. Morris,<sup>†</sup> Ken M. Page,<sup>†</sup> Lyn Rosenbrier Ribeiro,<sup>†</sup> Helen Sawney,<sup>†</sup> Stefan Steinbacher,<sup>‡</sup> Caroline Smith,<sup>†</sup> and Madeleine Vickers<sup>†</sup>

<sup>†</sup>AstraZeneca R&D, Mereside, Alderley Park, Macclesfield, Cheshire, SK10 4TG, U.K.

<sup>‡</sup>Proteros Biostructures, Am Klopferspitz 19, D-82152 Martinsried, Germany

## Supporting Information



**ABSTRACT:** Directed screening of nitrile compounds revealed **3** as a highly potent cathepsin K inhibitor but with cathepsin S activity and very poor stability to microsomes. Synthesis of compounds with reduced molecular complexity, such as **7**, revealed key SAR and demonstrated that baseline physical properties and in vitro stability were in fact excellent for this series. The tricyclic carboline P3 unit was discovered by hypothesis-based design using existing structural information. Optimization using small substituents, knowledge from matched molecular pairs, and control of lipophilicity yielded compounds very close to the desired profile, of which **34** (AZD4996) was selected on the basis of pharmacokinetic profile.

## INTRODUCTION

Osteoarthritis (OA) is made up of a group of degenerative disorders characterized by joint pain and loss of function in the absence of chronic autoimmune or autoinflammatory mechanisms.<sup>1</sup> With a global aging population, coupled with other risk factors such as obesity,<sup>2</sup> the disease represents a growing socioeconomic burden.<sup>3</sup> Pharmacological treatment is largely confined to symptomatic pain relief with intraarticular corticosteroid injection, analgesics, and NSAIDs,<sup>4</sup> to the point where, in severely advanced disease, joint replacement surgery is often performed, but is not always successful in alleviating pain and restoring function.<sup>5</sup> Articular cartilage breakdown is a prominent feature of joint degeneration and has consequently received significant attention from the pharmaceutical industry, where focusing on identifying targets, such as overexpressed proteases has led to drug development programs.

Cathepsin K (Cat K), a 24 kDa lysosomal cysteine protease, is expressed at high levels in osteoclasts and plays a key role in

bone resorption by degradation of type I cartilage.<sup>6</sup> Cat K knockout mice exhibit osteopetrosis (abnormally dense bone) of the long bones and vertebrae and abnormal joint morphology,<sup>7</sup> indicating the potential role of this enzyme in key bone pathologies associated with abnormal bone turnover such as osteoporosis (OP), osteoarthritis (OA), and metastatic bone disease (MBD).<sup>8–10</sup> As well as a role in bone disorders and OA, more recent findings have shown potential for the treatment of diabetes and obesity.<sup>11</sup>

Several pharmaceutical companies have trialed Cat K inhibitors in these disease areas; Novartis has completed phase II studies in OP and OA with balicatib (Figure 1).<sup>12</sup> The phase II OP trial reported positive outcomes on bone mineral density measures. Merck is studying odanacatib (MK0822) in a phase III trial for OP and has abandoned plans for a phase II in

Received: March 14, 2012

Published: June 28, 2012

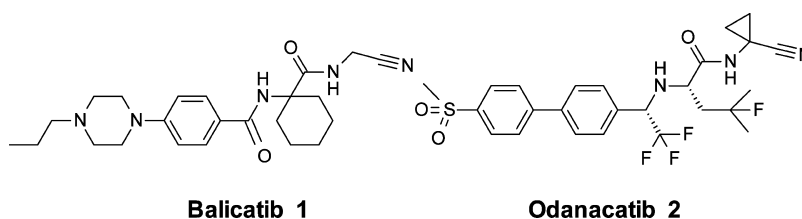


Figure 1. Literature nitrile cathepsin K inhibitors.

OA.<sup>13–15</sup> GSK (relacatib)<sup>16</sup> conducted phase I trials for both OP and OA several years ago but switched to MBD for phase II during 2006.<sup>17</sup>

**Drug-Hunting Approach.** A directed screen of nitrile-containing compounds, from the corporate collection, identified **3** and **4**, which were originally designed as inhibitors of cathepsin S (Cat S), as starting points for this work (Figure 2).<sup>18</sup> Both **3** (Cat K IC<sub>50</sub> 0.002 μM; Cat S IC<sub>50</sub> 0.076 μM) and

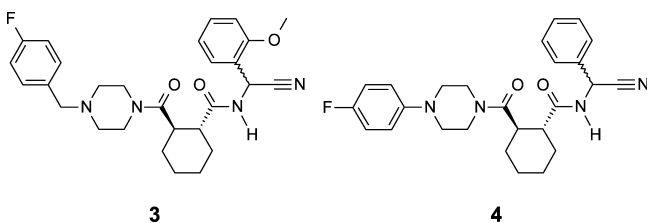


Figure 2. Screening hits from cathepsin S program.

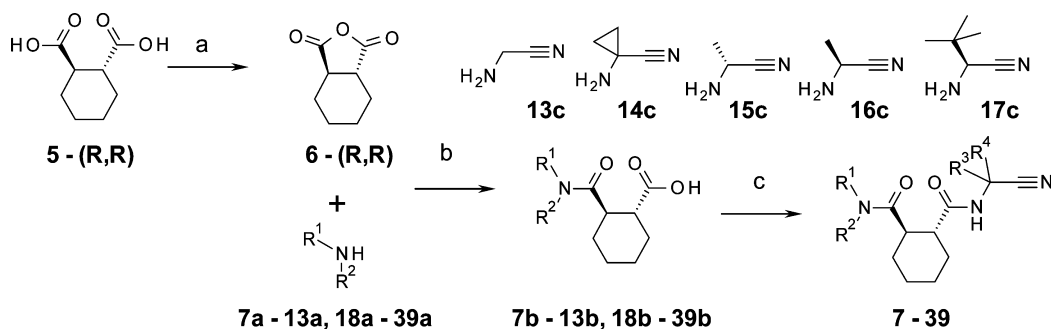
**4** (Cat K IC<sub>50</sub> 0.003 μM; Cat S IC<sub>50</sub> 0.258 μM) were attractive, potent neutral inhibitors of Cat K with some selectivity over Cat S. Cathepsins are present in the lysosome, an acidic compartment in cells, and as such basic compounds have been shown to accumulate to high concentration (lysotropism), resulting in pan cathepsin inhibition; hence, these neutral cyclohexyls are attractive from this point of view.<sup>19,20</sup> However, **3** and **4** both had poor metabolic stability in rodent pharmacokinetic (PK) studies, with clearances exceeding liver blood flow. The objective of the current study was to optimize these nitrile inhibitors by increasing Cat K selectivity and reduce metabolism to produce a PK profile compatible with oral dosing and an acceptable half-life.

We elected to start with an unsubstituted nitrile-amide covalent binder and selected simple tertiary amides with low molecular complexity.<sup>21</sup> There were two reasons for adopting this approach to library design. First, it was desirable to quantify

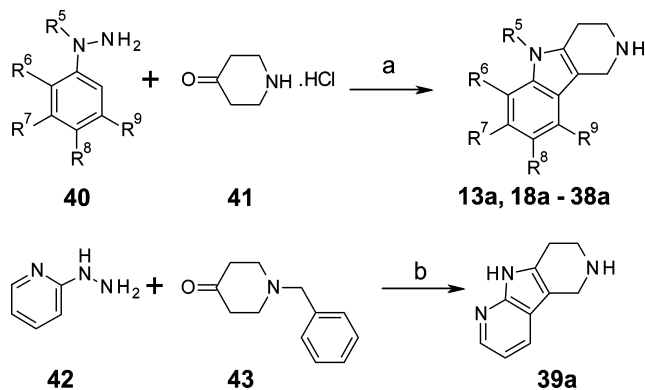
the contribution that the core portion of the molecule makes to affinity. Second, it was desirable to provide multiple scaffolds with hopefully high ligand efficiency (LE) that could readily be elaborated synthetically. The number of compounds in the design was further reduced, selecting those tertiary amides that would be rigid in structure and thereby most likely to make good surface contact with the protein surface, which is known to be fairly open in nature.<sup>22,23</sup> With this initial understanding of the SAR, these hopefully efficient scaffolds would allow exploration of the nitrile end of the molecules and then finally optimization to quality candidates.

**Chemistry.** The resolution of (±)-*trans*-cyclohexyl-1,2-dicarboxylic acid to yield (*R,R*)-**5** was initially carried out using (*R*)-1-phenethylamine by the method of Berkessel,<sup>24</sup> and subsequent recrystallizations gave a high enantiomeric excess (>99%). We found heating in neat acetic anhydride was a better method of dehydrating **5** into anhydride **6**, as this only required concentration to dryness to provide material used directly in the next step. Ring-opening of the anhydride at ambient temperature with a series of secondary amines (**7a–13a**, **18a–39a**) yielded in situ the acids **7b–13b**, **18b–39b** (Scheme 1). Final compounds (**7–39**) were synthesized by a general procedure of amide formation with the hydrochloride salt of aminoacetonitrile either with *O*-(7-azabenzotriazol-1-yl)-*N,N,N,N*-tetramethyluronium hexafluorophosphate (HATU) or benzotriazolyl-*oxy*-tris(pyrrolidino)phosphonium hexafluorophosphate (PYBOP) coupling reagents and diisopropylethylamine (DIPEA) at ambient temperature in overall yields of 7–78%. The carbolines used to synthesize final compounds were made by Fischer indole synthesis<sup>25</sup> from a suitable hydrazine **40** and 4-piperidone hydrochloride **41**. Simple heating of the two together in ethanol/concentrated HCl, in general, yielded the carboline in good yield (for example **34a**, R<sup>6</sup> = OCH<sub>3</sub> in 55%, Scheme 2). With electron-poor hydrazines, more forcing conditions from trifluoroboron etherate complex (BF<sub>3</sub>·OEt<sub>2</sub>) in acetic acid at 150 °C were used. The exception to this was

Scheme 1. Synthesis of Cyclohexyl-1,2-diamides **7–39**<sup>a</sup>



<sup>a</sup>Reagents and conditions: (a) Ac<sub>2</sub>O, 80 °C, 1 h, concentrate. (b) CH<sub>2</sub>Cl<sub>2</sub>, RT, 1 h, concentrate. (c) DMF or CH<sub>2</sub>Cl<sub>2</sub>, DIPEA (5 equiv), HATU (1.1 equiv), **13c–17c** HCl salts (1.0 equiv), RT, 12 h, 12–78% yield.

Scheme 2. Synthesis of Carbolines via Fischer Synthesis<sup>a</sup>

<sup>a</sup>Reagents and conditions: (a) (i) EtOH, concd HCl(aq), 80 °C, 3 h, 29–71% yield; or (ii) AcOH, BF<sub>3</sub>·OEt<sub>2</sub>, 80 °C, 3 h, 44–68% yield. (b) (i) PPA, 80 °C; (ii) HCO<sub>2</sub>H, NH<sub>4</sub>(HCO<sub>2</sub>), Pd(OAc)<sub>2</sub>, 40%.

the synthesis of 2,3,4,5-tetrahydro-1*H*-pyrido[4,3-*b*]-7-azaindole **35a** where an *N*-benzyl-protected 4-piperidone **39** with pyridine-1-hydrazine **38** and prolonged heating in polyphosphoric acid was required. Transfer hydrogenation using homogeneous conditions with palladium acetate, formic acid, and ammonium formate at reflux yielded **39a** in 40% overall yield on small scale only.<sup>26</sup> With these tricycles in hand, a similar procedure was followed to yield final SAR compounds by the same ring-opening method and coupling to the acid.

## RESULTS AND DISCUSSION

Enzyme inhibitory activity for seven compounds from this first library is reported in Table 1 with measured physicochemical properties and in vitro microsomal stability. The IC<sub>50</sub> value of 0.257 μM measured for the prototypical *N,N*-dimethyl amide **7** shows that the core substructure does indeed make a significant contribution to affinity and thus provides a useful reference point. The LE of 0.53 and ligand lipophilicity efficiency (LLE = -log<sub>10</sub>(IC<sub>50</sub>) - log D<sub>7.4</sub>) > 6 for **7** are both high, and the compound shows some good selectivity with respect to other cathepsins (Cat S, 14-fold). Compound **7** is polar (log D<sub>7.4</sub> < 0.5) and, as such, has good aqueous solubility and high stability in both human (HLM) and rat liver microsomes (RLM), revealing the cyclohexyl diamide core as an excellent chemical starting point.<sup>27–30</sup> Compared to **7**, partially and fully saturated rings with connecting aromatic rings yield positive gains in enzyme inhibition, which was in line with a concomitant rise in lipophilicity, suggesting hydrophobic and favorable ligand van de Waals interactions were responsible, and these were efficient (only slight reduction in LE on going from **7** to **13**). The change from **8** to **9** is interesting, suggesting an improved fit into the P3 groove by the partially saturated cyclohexenyl ring. The aromatic ring of **10** adds 9-fold in Cat K potency, suggesting only partial contact with the protein surface, but gratifyingly selectivity is improved (Cat S, 250 fold). (*N,N*)-Piperazines inspired by the original hits (**3**, **4**) were included in the library. Compound **11** is sufficiently basic to protonate at normal physiological pH, and the observation that it is

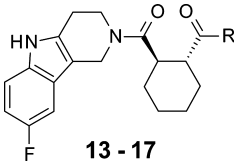
Table 1. SAR for Tertiary Amide Variations

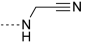
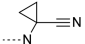
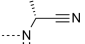
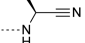
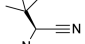
Compd	R <sup>1</sup> (R <sup>2</sup> )N	Cat K IC <sub>50</sub> <sup>a</sup> (μM)	Cat L IC <sub>50</sub> <sup>a</sup> (μM)	Cat S IC <sub>50</sub> <sup>a</sup> (μM)	Cat B IC <sub>50</sub> <sup>a</sup> (μM)	log D <sub>7.4</sub>	Mol W./Da	LE <sup>c</sup>	aqueous solubility pH 7.4 (μM)	HLM μL/min/mg <sup>d</sup>	RLM μL/min/mg <sup>e</sup>
<b>7</b>		0.257	>40	3.70	9.82	<0.5	237.3	0.53	>4600	5.1	<2.0
<b>8</b>		0.073	>100	2.11	8.75	0.9	277.4	0.49	>4900	<2.0	12
<b>9</b>		0.018 <sup>b</sup>	>100 <sup>b</sup>	ND	ND	0.9	275.4	0.53	>4900	4.5	41
<b>10</b>		0.002	3.11	0.515	0.712	1.9	325.4	0.50	360	23	145
<b>11</b>		0.037	>40	2.07	7.63	-0.1	292.4	0.48	3556	7.9	(<2)
<b>12</b>		0.007	>100	1.03	0.455	1.8	354.5	0.43	640	7.7	115
<b>13</b>		<0.001	>40	3.36	1.42	2.7	382.5	0.46	13	18	>250

<sup>a</sup>Binding affinity for cathepsin versus FRET substrate; mean of greater than *n* = 4 tests, unless where stated. <sup>b</sup>Mean of *n* = 2 tests. <sup>c</sup>kJ mol<sup>-1</sup> Da<sup>-1</sup>.

<sup>d</sup>In vitro human liver microsomal turnover mean of at least *n* = 2 tests (μL/min/mg). <sup>e</sup>In vitro rat liver microsomal turnover mean of at least *n* = 2 tests (μL/min/mg); values in parentheses denote rat liver hepatocyte Cl<sub>int</sub> mean *n* = 2 (μL/min/10<sup>6</sup> cells).

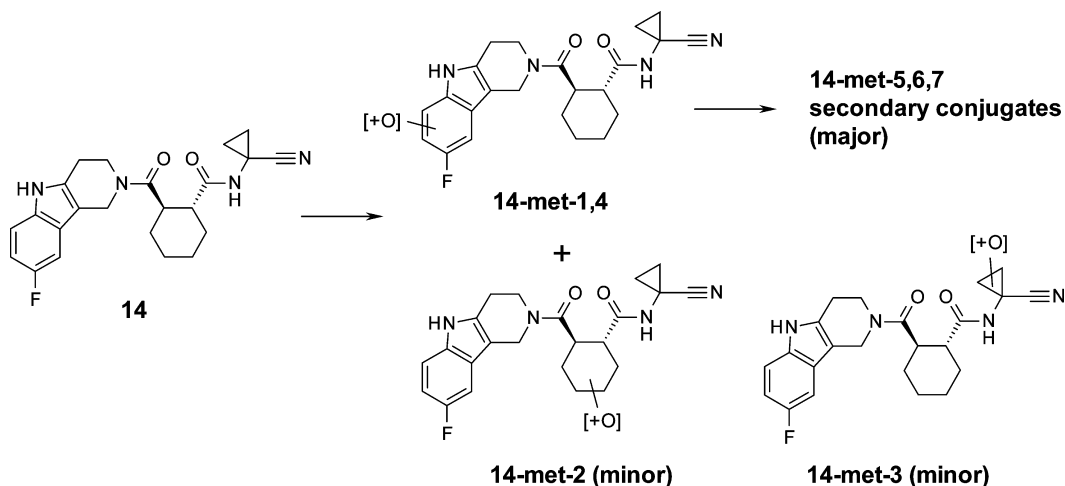
Table 2. SAR for Acetonitrile Substitutions



Compd	R - Nitrile	Cat K IC <sub>50</sub> <sup>a</sup> (μM)	Cat L IC <sub>50</sub> <sup>a</sup> (μM)	Cat S IC <sub>50</sub> <sup>a</sup> (μM)	Cat B IC <sub>50</sub> <sup>a</sup> (μM)	log <i>D</i> <sub>7,4</sub>	aqueous solubility pH 7.4 (μM)	HLM μL/min/mg <sup>c</sup>	RLM μL/min/mg <sup>d</sup>
13		<0.001	>40	3.36	1.42	2.7	13	18	>250
14		<0.001	>40	>6.6	3.52	3.0	580	41	>250
15		0.0162	>100	>100	44.9	3.1	460	12	>250
16		0.0173	>40	>70	73.5	3.5	-	-	-
17		0.785 <sup>b</sup>	>100 <sup>b</sup>	>100 <sup>b</sup>	31.2 <sup>b</sup>	>4.1	74	99	195

<sup>a</sup>Binding affinity Cat K versus FRET substrate; mean of greater than  $n = 4$  tests, unless where stated. <sup>b</sup>Mean of  $n = 2$  tests. <sup>c</sup>In vitro human liver microsomal turnover mean of at least  $n = 2$  tests ( $\mu\text{L}/\text{min}/\text{mg}$ ). <sup>d</sup>In vitro rat liver microsomal turnover mean of at least  $n = 2$  tests ( $\mu\text{L}/\text{min}/\text{mg}$ ).

Scheme 3. Metabolites Found after in Vitro Incubation of 14 with Rat Hepatocytes



essentially equipotent with **8** suggests that solvation of the cation is not compromised by binding to these proteins. Compound **9** again indicates that addition of a phenyl group increases potency to yield a lead similar to **10** but with lower selectivity (Cat S, 147 fold). The tricyclic carboline **13** stood out from this first library by having high enzyme inhibition (close to the tight binding limit for the assay<sup>31</sup>) and higher selectivity (Cat S, >3300; Cat B, >1400) despite compromised aqueous solubility and in vitro rat clearance.

The effects of substitution on the acetonitrile portion of the molecule were explored with compounds **14** through **17** to further develop the series from **13** (Table 2). Compound **14** is as potent as **13**, about 2-fold less stable in the in vitro HLM but 45-fold more soluble in water. This solubility difference is especially noteworthy because the latter is more lipophilic than the former. Enantiomers **15** and **16** are equipotent but over 10-

fold less potent against Cat K than either **13** or **14**. One interpretation of this observation is that **15** and **16** incur greater energy costs in adopting their bound positions in the protein. Similarly, the extra substitution of a methyl group on **15** had increased solubility. Increasing the bulk of the alkyl substituent appears to have an adverse effect on potency as shown by **17** Cat K IC<sub>50</sub> is ~800 fold less active.

Further testing of compound **14** found that high in vitro rat liver microsome turnover translated into high hepatocyte clearance and so explained the near liver blood flow clearance and low bioavailability; however, we did not rule out absorption as an additional contributing factor (Table 4). Thus, we examined **14** in iv and po dog pharmacokinetics and were encouraged to find that low in vitro translated into low in vivo clearance and pleasingly the bioavailability was high at 82%. While **14** is a good compound for further consideration the low

bioavailability in rodents left uncertainties about the human fraction absorbed so we sought to optimize clearance in rodents while maintaining a good dog PK. Metabolite identification from *in vitro* rat hepatocyte incubation of **14** highlighted that an oxidation event occurred on the cyclohexyl ring (**14-met-2**), as has been reported for structurally related compounds (Scheme 3).<sup>22</sup> However, major metabolites were found from oxidation on the carboline ring and subsequent conjugation (**14-met-1, -4, -5, -6, -7**), suggesting that substitution on this ring may lead to reduced metabolism.

The structure of a cocrystal of **14** with Cat K revealed a covalent bond between the nitrile of **14** and the active site C25 as the primary interaction, with the primary amide group forming hydrogen bonds to N161 and G66, as has been observed in related inhibitor complexes (Figure 3A).<sup>32</sup> The

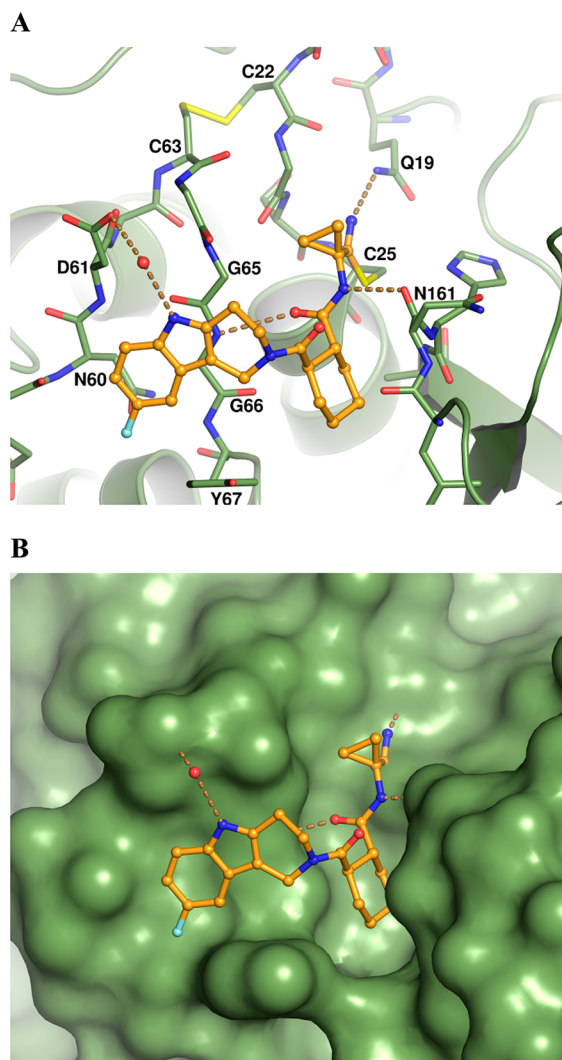


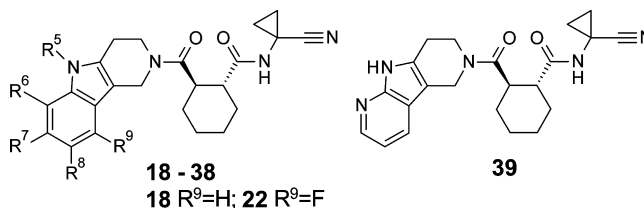
**Figure 3.** Compound **34** bound to cathepsin K (PDB 4DMY). (A) Identification of key H-bonding residues. (B) Surface of protein to illustrate the fit of the cyclohexyl and carboline moieties.

cyclohexane ring of a related inhibitor has been shown to occupy the relatively shallow S2 pocket of the enzyme as does **14** (seen more clearly in Figure 3B).<sup>22,23</sup> The tricyclic carboline fits into a relatively flat open S3 groove, bound on one side by a glycine-rich loop and Y67 on the other side, such that an aromatic C–H (R9) is placed against it. The solvent-exposed

acid moiety of D61 was measured in this static structure at 3.95 Å from the carboline N–H (R5), suggesting a possible hydrogen bond; however, both groups are exposed to solvent so this is unlikely to contribute significantly to binding free energy. The fluoro atom at R8 does not appear to make much surface contact, and the structure suggests space to expand along the protein surface. From these findings we decided to explore SAR at R5, R6, R7, and R8, of the carboline, leaving R9 unsubstituted to maintain the interaction with Y67, monitoring the effects on potency and aiming to reduce metabolism using the *in vitro* RLM assay (Table 3). With LE and LLE already high for **14**, we focused on small substituents or heteroatom substitution to combine SAR exploration and potential metabolic blocks, while keeping lipophilicity under control to retain aqueous solubility. The structural prototype **18** was synthesized first and was nearly equipotent to **14**, with almost millimolar aqueous solubility. A fluorine scan (**19** to **21** and including **14**) revealed that binding to Cat K compromised fluorination at positions R7 and R9 although this substituent can be accommodated without loss of potency at positions R6 and R8. Of these four compounds, **20**, the least potent, was the only compound with a significant increase in RLM stability. Addition of a methyl at **22** (or N–H of carboline) resulted in a small drop in activity consistent with the hypothesis that the N–H did not form a H-bond to D61. Despite the initial hypothesis, increasing the size of the group at R8 resulted in a decrease in Cat K inhibition (**23** to **27**); we speculate that the bulky groups have moved the tricyclic out of the groove such that the R9 is further from Y67. The target protein is more tolerant of larger substituents at R6 (**29**–**38**), although none of these led to a significant increase in potency relative to **18**. From the structure of **14** bound in Cat K, these groups would point out to solvent and should make an impact on inhibition: chloro **29**, methyl **30**, bromo **31**, and CF<sub>3</sub> **33** are all less active, despite being more lipophilic, and did not alter RLM clearance. Lipophilicity is generally associated with poor ADMET characteristics so we included polar substituents into our compound design.<sup>33</sup> The CH<sub>3</sub>SO<sub>2</sub> substituent, which often improves the physicochemical properties of compounds<sup>34</sup> and HLM stability,<sup>35,36</sup> was introduced at three positions (**27**, **28**, and **38**). Although this led to significantly increased stability in both HLM and RLM assays, the accompanying loss of potency was unacceptably large. Similarly, the 6-CN compound **32** was predicted to increase stability and yielded a significant reduction in RLM (80 μL/min/mg) and a small reduction in measured log *D*<sub>7.4</sub> and was similar in Cat K potency. However, the 6-OCH<sub>3</sub> (**34**, IC<sub>50</sub> < 0.001 μM) and 6-OCF<sub>3</sub> (**36**, IC<sub>50</sub> 0.002 μM) were more stable in HLM and RLM assays despite the increase in lipophilicity, and comparing to 6-SCH<sub>3</sub> **35**, which showed a small reduction in activity, and 6-OCH<sub>2</sub>CH<sub>3</sub>, we observed that the alkoxy substituent had an electronic effect that maintained high Cat K activity and increased stability. Finally, we synthesized 6-aza-carboline **39** following the SAR that the 6 position tolerated substitution and allowed reduction in lipophilicity. As hypothesized, the compound has improved stability in both RLM and HLM stability but without any reduction of Cat K potency.

Table 4 has comparison data for **14**, **34**, and **39** obtained from *in vitro* assay and *in vivo* rat and dog PK experiments, including scaling to human predicted data.<sup>37,38</sup> Plasma protein binding was not an issue because the fraction unbound exceeded 10% in rat, dog, and human plasma. The increase in the *in vitro* stability for **34** translated into improved

Table 3. SAR for Carboline Substitutions



compd	R5	R6	R7	R8	Cat K IC <sub>50</sub> <sup>a</sup> ( $\mu$ M)	log D <sub>7.4</sub>	aqueous solubility, pH 7.4 ( $\mu$ M)	HLM $\mu$ L/min/mg <sup>c</sup>	RLM $\mu$ L/min/mg <sup>d</sup>
18	H	H	H	H	0.001	2.7	910	26	143
19	H	F	H	H	<0.001	3.0	470	55	311
20	H	H	F	H	0.004	3.0	540	36	89
14	H	H	H	F	<0.001	3.0	580	41	>250
21	H	H	H	H	0.010	3.2	128	57	322
22	CH <sub>3</sub>	H	H	F	0.003	2.8	300	170	>350
23	H	H	H	Cl	0.003	3.7	130	87	>350
24	H	H	H	CH <sub>3</sub> O	0.041	2.4	822	29	(20)
25	H	H	H	CF <sub>3</sub>	0.042 <sup>b</sup>	4.2	74	33	82
26	H	H	H	(CH <sub>3</sub> ) <sub>2</sub> CH	0.050 <sup>b</sup>	4.1	84	—	—
27	H	H	H	CH <sub>3</sub> SO <sub>2</sub>	0.078 <sup>b</sup>	—	193	14	(3.5)
28	H	H	CH <sub>3</sub> SO <sub>2</sub>	H	0.034 <sup>b</sup>	1.5	902	<2.0	7.2
29	H	Cl	H	H	0.002	3.6	210	46	226
30	H	CH <sub>3</sub>	H	H	0.003	3.0	510	25	179
31	H	Br	H	H	0.004	3.1	140	43	164
32	H	N $\equiv$ C	H	H	0.002 <sup>b</sup>	2.5	400	34	80
33	H	CF <sub>3</sub>	H	H	0.005 <sup>b</sup>	3.8	150	26	116
34	H	CH <sub>3</sub> O	H	H	<0.001	2.7	620	16	67
35	H	CH <sub>3</sub> S	H	H	0.004	—	—	79	303
36	H	CF <sub>3</sub> O	H	H	0.002	4.0	120	19	53
37	H	CH <sub>3</sub> CH <sub>2</sub> O	H	H	<0.001	3.1	300	13	62
38	H	CH <sub>3</sub> SO <sub>2</sub>	H	H	0.017	1.7	1600	4.0	23
39					0.001	2.1	1500	12	25

<sup>a</sup>Binding affinity Cat K versus FRET substrate; mean of greater than  $n = 4$  tests, unless where stated. Compounds tested at least  $>4 \mu$ M for Cat S,  $>2.9 \mu$ M for Cat B and as inactive for Cat L. <sup>b</sup>Mean of  $n = 2$  tests. <sup>c</sup>In vitro human liver microsomal turnover mean of at least  $n = 2$  tests ( $\mu$ L/min/mg). <sup>d</sup>In vitro rat liver microsomal turnover mean of at least  $n = 2$  tests ( $\mu$ L/min/mg); values in parentheses for rat liver hepatocyte Cl<sub>int</sub> mean  $n = 2$  ( $\mu$ L/min/10<sup>6</sup> cells).

Table 4. Serum Protein Binding and Pharmacokinetic Data

compd	species	protein binding (% free) <sup>a</sup>	in vitro hepatocyte Cl <sub>int</sub> ( $\mu$ L/min/10 <sup>6</sup> cells)	Cl <sub>p</sub> (mL/min/kg)	V <sub>dss</sub> (L/kg)	iv half-life (h)	bioavailability (%)
14	rat	16	126 $\pm$ 28	63 $\pm$ 7.8 <sup>b</sup>	2.3 $\pm$ 0.3	0.6 $\pm$ 0.2	3.8 $\pm$ 2.1
	dog	13	6.7 ( $n = 1$ )	10 $\pm$ 4.9 <sup>c</sup>	1.2 $\pm$ 0.5	1.8 $\pm$ 0.2	82 $\pm$ 21
	human	14	<2.5 ( $n = 2$ )	[<5.3] <sup>d</sup>	[1.7]	[3.7]	[40]
34	rat	17	23 $\pm$ 16	53 $\pm$ 3.4 <sup>b</sup>	2.3 $\pm$ 0.3	1.0 $\pm$ 0.08	28 $\pm$ 12
	dog	22	2.5 $\pm$ 2.3	10 $\pm$ 2.4 <sup>c</sup>	1.7 $\pm$ 0.4	1.5 $\pm$ 0.06	65 $\pm$ 5.1
	human	17	5.3 $\pm$ 4.6	[8.7] <sup>d</sup>	[2.0]	[2.2]	[53]
39	rat	42	9.9 $\pm$ 7.9	32 $\pm$ 9.7 <sup>b</sup>	1.6 $\pm$ 0.6	1.8 $\pm$ 0.8	12 $\pm$ 3.7
	dog	38	3.1 $\pm$ 1.0	7.2 $\pm$ 4.8 <sup>c</sup>	0.9 $\pm$ 0.1	1.4 $\pm$ 0.4	59
	human	33	<2.0 ( $n = 6$ )	[<5.4] <sup>d</sup>	[1.0]	[2.1]	[42]

<sup>a</sup>All results are a mean at least  $n = 2$  experiments. All pharmacokinetic experiments reported as single dosed compounds in at least two experiments involving two animals in each. <sup>b</sup>Alderley Park Han Wistar male rats, dosed to fed animals, po 2.0 mg/kg as a suspension in 5% DMSO/95% HPMC/TWEEN, iv dosed as solution in 40% DMA/water at 2.0 mg/kg. <sup>c</sup>Beagle dog, dosed to fasted animals, po 1.0 mg/kg as a suspension in 5% DMSO/95% HPMC/TWEEN, iv dosed as solution in 10% DMSO/90% Sorensens at 1.0 mg/kg. <sup>d</sup>Numbers inside brackets are predicted values from scaling to human from rat and dog results; see Supporting Information.

bioavailability in rat (28%), which was maintained in dogs (65%). The in vitro human hepatic clearance of 39 was consistently below the limit of detection, rat hepatic clearance was low at 9.9  $\mu$ L/min/10<sup>6</sup> cells, and this led to a prediction of low clearance in vivo; however, we observed a CL of 32 mL/min/kg. Metabolite identification of rat urine after oral dosing found a significant number of metabolites and parent

compound (ca. 50% of total clearance).<sup>39</sup> When scaled to human, this extra component is likely to cause an approximate 30% increase in the human clearance.<sup>40</sup> The consequent decrease in human half-life made it unlikely that the compound would be a suitable clinical candidate. For compound 34, neither in vitro human hepatic Cl<sub>int</sub> (predicted low clearance) nor rodent renal elimination data (not detectable) suggested

Scheme 4. Metabolites Found after in Vitro Incubation of 34 with Rat Hepatocytes

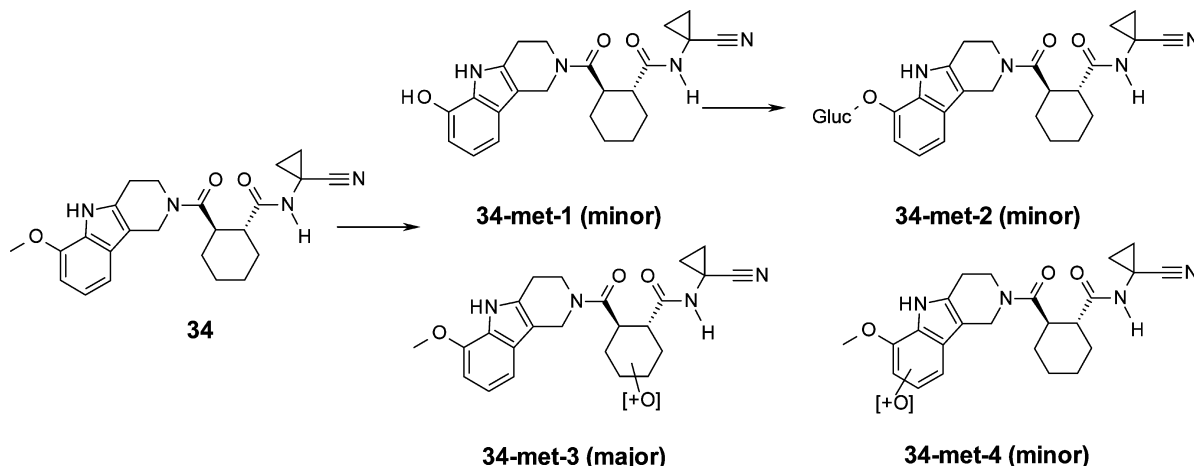
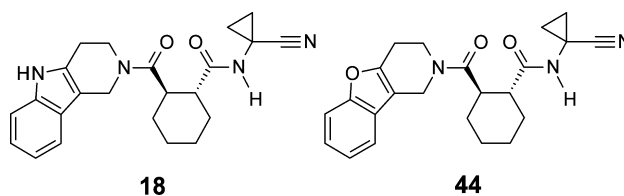


Table 5. SAR for Carboline Substitutions



compd	Cat K IC <sub>50</sub> (μM)	log D <sub>7.4</sub>	aqueous solubility, pH 7.4 (μM)	protein binding (% free) <sup>a</sup>	RLM (μL/min/mg) <sup>b</sup>	Cl <sub>p</sub> (mL/min/kg)	bioavailability (%)
18	0.004	2.7	910	23	143	46 ± 7.9 <sup>c</sup>	8.2 ± 5.1
44	0.025	3.0	580	12	>350	52 (n = 1)	0.0 (n = 1)

<sup>a</sup>All results are a mean of at least  $n = 2$  experiments. <sup>b</sup>In vitro rat liver microsomal turnover mean of at least  $n = 2$  tests (μL/min/mg). <sup>c</sup>All pharmacokinetic experiments reported as single dosed compounds in at least two experiments involving two animals in each. Alderley Park Han Wistar male rats, dosed to fed animals, po 2.0 mg/kg as a suspension in 5% DMSO/95% HPMC/TWEEN, iv dosed as solution in 40% DMA/water at 2.0 mg/kg.

that human clearance would be a risk; this plus the consistency in oral absorption observed across species for the compound confirmed it as a more likely clinical candidate.

To understand the effect of the OCH<sub>3</sub> group at R6 on pharmacokinetic properties, metabolites of 34 post in vitro incubation with rat hepatocytes were examined. This showed a switch of major metabolite to oxidation of the cyclohexyl ring (34-met-3) and reduced oxidation of the carboline aromatic (34-met-4) (Scheme 4) when compared to 14 (Scheme 3). A new metabolic route by oxidative demethylation and conjugation was found (34-met-1 and -2) although they were minor metabolites. This change in profile resulted in an overall reduction in rate of turnover, perhaps by a change in recognition by the Cyp450s involved. We also considered that the effect of the OCH<sub>3</sub> was to partially mask the N–H donor of the carboline group. Reduction of the number of hydrogen bond donors is an adopted approach for improving pharmacokinetics and, in particular, absorption.<sup>41–44</sup> As such, compound 44 would test this hypothesis by complete removal of the donor and could be compared with the unfunctionalized carboline 18 (Table 5). Surprisingly, 44 had high in vitro rat microsomal turnover and no bioavailability; in comparison, 18 had low bioavailability and high clearance, marking it hard to establish the role of the H-bond donor of the carbolines from a pharmacokinetic point of view.

**In Vivo Pharmacology.** The in vivo effects of 34 were studied in dogs using levels of C-telopeptide (CTX-1), a

protein fragment of type 1 collagen, as a measure of Cat K inhibition.<sup>45–47</sup> Compound 34 tested in a dog Cat K enzyme FRET assay had a mean inhibition IC<sub>50</sub> of 0.8 nM ( $n = 7$ ), the same as human enzyme inhibition. Blood level concentrations of 34 and CTX-1 were measured as a function of time in this PK/PD study at three doses (0.1, 0.3, and 2.0 mg/kg), the results of which are summarized in Figure 4. A dose-dependent increase in the area under the curve was observed (Figure 4a) and concomitant reduction in [CTX-1] which appeared very similar at the three doses studied (Figure 4b). This clearly demonstrated target engagement, rapid onset of action, and the in vivo potency of 34; a maximum effect level has been reached with all three doses. These data suggest that inhibition of Cat K need only occur for a short period of time to achieve maximum inhibition.

## CONCLUSION

Directed screening of nitrile compounds revealed 3 and 4 as highly potent cathepsin K (Cat K) inhibitors but with Cat S activity and very poor stability to microsomes. Reducing molecular complexity led to compounds such as 7 that revealed key SAR and demonstrated that baseline physical properties and in vitro stability were in fact excellent for this series. The tricycle carboline P3 unit was discovered by hypothesis-based design using existing structural information. Optimization using small substituents, knowledge from matched molecular pairs, and control of lipophilicity yielded compounds very close to the

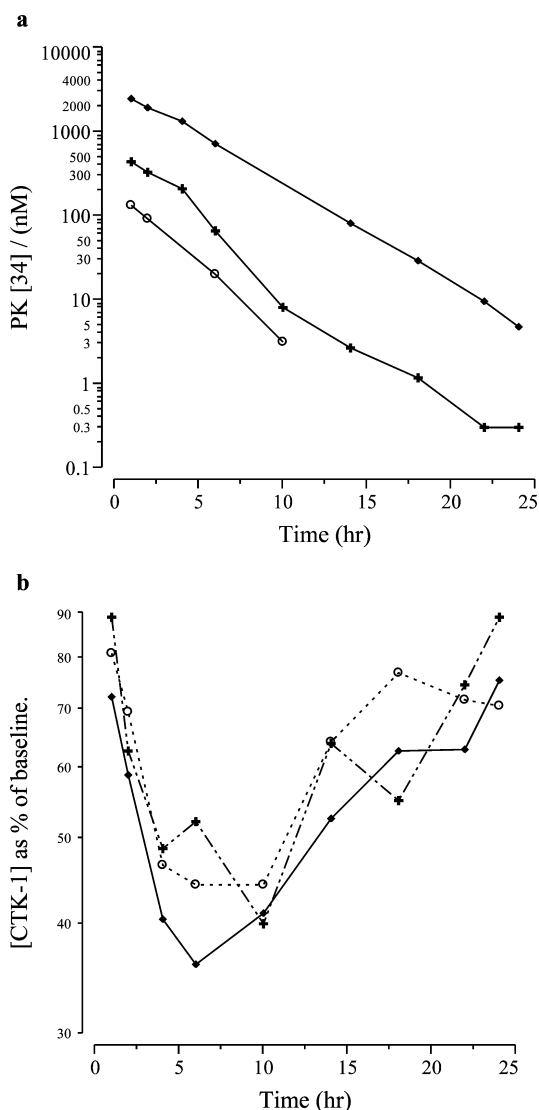


**Figure 4.** Dog PK/PD experiment for compound 34. Each point was mean  $n = 2$  with the same blood sample taken at a given time after compound dosing split to measure [34] and [CTX-1]. (a) Total plasma [34] from the dog PK experiment: O, PK[34]/nM at 0.1 mg/kg uid; +, PK[34]/nM at 0.3 mg/kg uid/nM; ◆, PK[34]/nM at 2.0 mg/kg uid. (b) ELISA-measured reduction [CTX-1] from baseline: O, [CTX-1] as % baseline 0.1 mg/kg uid; +, [CTX-1] as % baseline 0.3 mg/kg uid; ◆, [CTX-1] as % baseline 2.0 mg/kg uid.

desired profile, such as 39. We were surprised to find an  $\text{OCH}_3$  at R6 (34) had reduced metabolic turnover and thus improved pharmacokinetics in rodents, as well as the benefit of a simple high-yielding synthesis. The  $\text{OCH}_3$  group also retained Cat K inhibition, although the mechanism for this and the increased stability are not understood. Selectivity was also maximized with only Cat B inhibition observed at  $2.97 \mu\text{M}$  (>3000 fold) and hERG ionworks screening inactive (>100  $\mu\text{M}$ ). Comparing to balicatib, synthesized and tested in our hands (Cat K  $0.005 \mu\text{M}$ , Cat B  $4.75 \mu\text{M}$ ), and bdanacatib (Cat K <0.001  $\mu\text{M}$ , Cat S  $0.183 \mu\text{M}$ ), we found our compounds as potent but with higher selectivity. Our in vivo pharmacology experiment in dogs demonstrated target engagement and a maximum inhibition of activity at 0.1 mg/kg, showing the potential of this compound as a clinical candidate. Considering all of these factors and the

short convergent route, compound 34 (AZD4996) was selected as a clinical candidate.

## EXPERIMENTAL SECTION

All solvents and chemicals used were reagent grade. Anhydrous solvents tetrahydrofuran (THF) and dimethoxyethane (DME) were purchased from Aldrich. Purity and characterization of compounds were established by a combination of low resolution mass spectra (LC-MS), obtained using a Waters liquid chromatography mass spectrometry system, where purity was determined by UV absorption at a wavelength of 254 nm and the mass ion determined by electrospray ionization (Micromass instrument), and NMR analytical techniques. All test compounds were >95% pure.  $^1\text{H}$  NMR spectra were recorded using a AVIAN AV400 FT spectrometer or via a Flow NMR process using an AVANCE 500 FT spectrometer.  $\text{DMSO}-d_6$  or  $\text{CDCl}_3$  solvent was used, with the data expressed as chemical shifts in ppm from internal standard TMS on the  $\delta$  scale. Coupling constants ( $J$ ) values are reported in hertz (Hz). Splitting patterns are indicated as follows: s, singlet; d, doublet; t, triplet; m, multiplet; br, broad peak. Compounds 7, 11, 12, and 14–27 when measured by  $^1\text{H}$  NMR at ambient temperature showed differential rotameric peaks around the tertiary amide group. In these cases, assignments for protons which were measured distinctly have been expressed as fractions (e.g., 0.5H). Higher temperature  $^1\text{H}$  NMR spectra have been recorded on compounds 13, 14, and 39 for comparison and clear assignment. The reverse phase column used was a 4.6 mm  $\times$  50 mm Phenomenex Synergi Max-RP 80 Å, and the solvent system was water containing 0.1% formic acid and acetonitrile unless otherwise stated. A typical run was 5.5 min with a 4.0 min gradient from 0% to 95% acetonitrile. Purification by column chromatography was typically performed using silica gel (Merck 7734 grade) and solvent mixtures, and gradients are described herein. Purification by reverse phase high performance chromatography was typically performed using a Perkin-Elmer instrument using UV detection at 254 nm and a C18 1500  $\times$  21.2 mm Phenomenex column 100 Å. Acidic conditions (0.1% to 0.5% formic acid) or basic conditions (ammonia to pH 10) were used with gradient solvent mixtures of acetonitrile and water. SCX columns were supplied from International Sorbent Technology and used as directed in this specific case.

**General Procedure for the Preparation of 7, 12–14, 34, and 39.** An appropriate amine (1.0 equiv) was added to (3aR,7aR)-hexahydroisobenzofuran-1,3-dione (6) (1.0 equiv) and DIPEA (3.0 equiv) in  $\text{CH}_2\text{Cl}_2$  to a concentration of 0.1 M. The resulting solution was stirred at 20 °C for 18 h and then either aminoacetonitrile hydrochloride (13c) or 14c (3.0 equiv) was added followed by HATU (1.1 equiv) and further DIPEA (5.0 equiv). The resulting suspension was stirred at 20 °C for 72 h. The solution was diluted with  $\text{CH}_2\text{Cl}_2$  (equal volume), partitioned with 50% brine (equal volume), dried ( $\text{Na}_2\text{SO}_4$ ), concentrated in vacuo, and adsorbed onto silica. Flash chromatography (silica, 0–100% EtOAc in isohexane) yielded the desired compound, usually as a solid, or alternatively preparative HPLC was used where stated.

**(1R,2R)-N-(Cyanomethyl)-N,N-dimethylcyclohexane-1,2-dicarboxamide (7).** Dimethylamine (2 M in THF, 0.65 mL, 1.30 mmol) was utilized with 1-aminoacetonitrile hydrochloride (192 mg, 2.08 mmol) (13c) to yield 7, after purification via prep HPLC, as a white powder (192 mg, 61%). HRMS (ES+) for  $\text{C}_{12}\text{H}_{20}\text{O}_2\text{N}_3$  ( $\text{M}^+ + \text{H}$ ): calcd 238.1550; found, 238.1551.  $^1\text{H}$  NMR (400 MHz,  $\text{CDCl}_3$ )  $\delta$  1.21–1.48 (m, 4H), 1.48–1.67 (m, 1H), 1.67–2.00 (m, 4H), 2.70 (ddd,  $J = 12.5, 10.6, 3.6$  Hz, 1H), 2.82–2.96 (m, 4H), 3.08 (s, 3H), 3.99 (dd,  $J = 17.4, 5.9$  Hz, 1H), 4.10 (dd,  $J = 17.4, 5.9$  Hz, 1H), 7.09 (s, 1H).

**(1R,2R)-N-(Cyanomethyl)-2-(4-phenylpiperazine-1-carbonyl)cyclohexanecarboxamide (12).** N-(4-Phenyl)piperazine (162 mL,  $\sim 1.0$  mmol) was utilized with 1-aminoacetonitrile hydrochloride (29.0 mg, 0.52 mmol) (13c) to yield 12, after purification via prep HPLC, as a solid gum (80.3 mg, 52%). HRMS (ES+) for  $\text{C}_{20}\text{H}_{27}\text{O}_2\text{N}_4$  ( $\text{M}^+ + \text{H}$ ): calcd 355.2129; found, 355.2130.  $^1\text{H}$  NMR (500 MHz, DMSO)  $\delta$  1.11–1.50 (m, 4H), 1.62–1.92 (m,



4H), 2.58 (t,  $J = 16.0$  Hz, 1H), 2.94 (t,  $J = 16.0$  Hz, 1H), 3.01–3.27 (m, 4H), 3.59–3.70 (m, 4H), 4.05 (d,  $J = 5.6$  Hz, 2H), 6.81 (t,  $J = 7.2$  Hz, 1H), 6.94 (d,  $J = 7.2$  Hz, 2H), 7.23 (t,  $J = 7.2$  Hz, 2H), 8.49 (t,  $J = 5.6$  Hz, 1H).

**(1R,2R)-N-(Cyanomethyl)-2-(8-fluoro-1,3,4,5-tetrahydropyrido[4,3-b]indole-2-carbonyl)-cyclohexanecarboxamide (13).** 8-Fluoro-1,3,4,5-tetrahydropyrido[4,3-b]indole **13a** (162 mg, 0.87 mmol) was utilized with 1-aminoacetonitrile hydrochloride (69.0 mg, 0.75 mmol) (**13c**) to yield **13**, after purification via prep HPLC, as a solid gum (134 mg, 57%). HRMS (ES+) for  $C_{21}H_{24}O_2N_4F$  ( $M^+ + H$ ): calcd 383.1878; found, 383.1880.  $^1H$  NMR (500 MHz, DMSO)  $\delta$  1.13–1.50 (m, 4H), 1.62–1.92 (m, 4H), 2.58 (t,  $J = 10.4$  Hz, 1H), 2.75–3.09 (m, 4H), 3.48–3.75 (m, 3H), 4.00–4.16 (m, 2H), 6.88 (d,  $J = 3.8$  Hz, 2H), 6.97 (dt,  $J = 13.7, 5.9$  Hz, 2H), 8.48 (t,  $J = 5.5$  Hz, 1H).  $^1H$  NMR (500 MHz, DMSO)  $\delta$  1.18–1.48 (m, 4H), 1.62–1.91 (m, 4H), 2.79 (t,  $J = 11.7$  Hz, 1H), 2.75–2.93 (m, 2H), 3.03 (t,  $J = 11.7$  Hz, 1H), 3.80 (s, 1H), 3.87–4.06 (m, 2H), 4.64 (t,  $J = 16.6$  Hz, 2H), 6.83 (td,  $J = 9.2, 2.4$  Hz, 1H), 7.20 (d,  $J = 7.0$  Hz, 1H), 7.25 (dd,  $J = 8.7, 4.5$  Hz, 1H), 8.08 (s, 1H), 10.64 (s, 1H).

**(1R,2R)-N-(1-Cyanocyclopropyl)-2-[(8-fluoro-1,3,4,5-tetrahydro-2H-pyrido[4,3-b]indol-2-yl)carbonyl]-cyclohexanecarboxamide (14).** **13a** (798 mg, 4.20 mmol) was utilized with **14c** (585 mg, 5.04 mmol) to yield **14**, after purification silica chromatography, as a solid gum (212 mg, 12%). HRMS (ES+) for  $C_{23}H_{26}O_2N_4F$  ( $M^+ + H$ ): calcd 409.2034; found, 409.2036.  $^1H$  NMR (400 MHz,  $CDCl_3$ )  $\delta$  0.77–0.94 (m, 1H), 0.95–1.54 (m, 7H), 1.75–1.91 (m, 4H), 2.61 (“t”,  $J = 11.4$  Hz, 1H), 2.68–2.94 (m, 3H), 3.64–3.80 (m, 1H), 3.88–4.03 (m, 0.5H), 4.20–4.33 (m, 0.5H), 4.60 (d,  $J = 15.7$  Hz, 0.5H), 4.69 (s, 1H), 4.89 (d,  $J = 15.8$  Hz, 0.5H), 6.53 (s, 0.5H), 6.61 (s, 0.5H), 6.89 (td,  $J = 11.3, 2.4$  Hz, 1H), 7.08 (td,  $J = 9.4, 2.3$  Hz, 1H), 7.20 (td,  $J = 8.8, 2.3$  Hz, 1H), 7.93 (s, 1H).  $^1H$  NMR (500 MHz, DMSO)  $\delta$  0.88 (s, 1H), 1.01 (s, 1H), 1.19–1.45 (m, 6H), 1.70–1.85 (m, 4H), 2.79–2.90 (m, 2H), 3.01 (td,  $J = 11.9, 3.6$  Hz, 1H), 3.81 (s, 1H), 3.88 (dt,  $J = 11.3, 5.7$  Hz, 1H), 4.63 (s, 2H), 6.82 (dt,  $J = 9.2, 2.6$  Hz, 1H), 7.22 (d,  $J = 9.2$  Hz, 1H), 7.26 (dd,  $J = 8.8, 4.6$  Hz, 1H), 8.26 (s, 1H), 10.65 (s, 1H).

**6-Methoxy-2,3,4,5-tetrahydro-1H-pyrido[4,3-b]indole (34a).** Piperidin-4-one hydrochloride (**41**) (4.66 g, 34.5 mmol) was added to a suspension of (2-methoxyphenyl)hydrazine hydrochloride (6.00 g, 34.4 mmol) in ethanol (80 mL) and concd HCl (6.0 mL), and the resulting solution was heated at 80 °C for 3 h. The reaction was allowed to cool to room temperature overnight, and the resulting precipitated solid was filtered, washed with chilled ethanol (20 mL), and dried under vacuum to give a salt. This was stirred in water (100 mL) and made basic with 2 M NaOH(aq) (~5 mL), and the resulting solid was filtered, azeotroped with toluene (30 mL, rotary evaporator), and dried under vacuum to yield **34a** (3.84 g, 55%) as an off-white solid. LCMS (+ve ESI):  $t_R = 0.85$  min, 203.3 ( $M + H$ )<sup>+</sup>.  $^1H$  NMR (400 MHz, DMSO) 2.63–2.66 (m, 2H), 2.99–3.03 (m, 2H), 3.83 (‘s’, 2H), 3.89 (s, 3H), 6.59 (d,  $J = 7.5$  Hz, 1H), 6.83 (“t”,  $J = 7.8$  Hz, 1H), 6.93 (d,  $J = 7.8$  Hz, 1H), 10.72 (s, 1H).

**(1R,2R)-N-(1-Cyanocyclopropyl)-2-[(6-methoxy-1,3,4,5-tetrahydro-2H-pyrido[4,3-b]indol-2-yl)carbonyl]-cyclohexanecarboxamide (34).** **34a** (3.84 g, 19.0 mmol) was utilized with 1-aminocyclopropanecarbonitrile hydrochloride **14c** (6.76 g, 57.0 mmol) to yield **34** after purification via flash silica chromatography and crystallization slurry stirring over 48 h (6.27 g, 78%) as a white powder. HRMS (ES+) for  $C_{24}H_{29}O_3N_4$  ( $M^+ + H$ ): calcd 421.2234; found, 421.2233.  $^1H$  NMR (400 MHz, DMSO)  $\delta$  0.73–0.83 (m, 1H), 0.87–0.91 (m, 0.5H), 0.87–1.03 (m, 1H), 1.17–1.40 (m, 6H), 1.61–1.82 (m, 5H), 2.63–2.70 (m, 1H), 2.75–2.82 (m, 0.5H), 2.84–3.05 (m, 1.5H), 3.64–3.72 (m, 0.5H), 3.94–3.73 (m, 5H), 4.71 (s, 1H), 6.64 (“t”,  $J = 8.2$  Hz, 1H), 6.90 (qn,  $J = 7.8$  Hz, 1H), 6.97 (d,  $J = 7.8$  Hz, 0.5H), 7.10 (d,  $J = 7.8$  Hz, 0.5H), 8.64 (s, 1H), 10.91 (s, 1H).

**1-Benzylpiperidin-4-one Pyridin-2-yl Hydrazone (45).** 2-Hydrazinopyridine dihydrochloride (5.00 g, 27.5 mmol) and 1-benzylpiperidin-4-one (6.18 g, 27.5 mmol) were suspended in EtOH (70 mL). AcOH (2 mL) was added and the mixture stirred at reflux

for 2 h, cooled to RT, and concentrated in vacuo. The residue was partitioned between 2 N NaOH (aq) (10 mL) and  $CH_2Cl_2$  ( $2 \times 30$  mL), and the combined organic fractions were dried ( $Na_2SO_4$ ), concentrated in vacuo, and adsorbed onto silica for purification by flash column chromatography (0–10% MeOH/ $CH_2Cl_2$ ). This gave **45** as a pale yellow gum which was used crude in the next reaction (7.70 g, 100% yield).  $^1H$  NMR (400 MHz, DMSO)  $\delta$  2.34 (d,  $J = 5.6$  Hz, 2H), 2.62–2.36 (m, 6H), 3.52 (s, 2H), 6.68 (ddd,  $J = 7.1, 4.9, 0.8$  Hz, 1H), 7.04 (s, 1H), 7.51–7.06 (m, 5H), 7.59–7.51 (m, 1H), 8.05 (dd,  $J = 4.9, 1.1$  Hz, 1H), 9.47 (s, 1H).

**N-Benzyl-2,3,4,5-tetrahydro-1-benzylpyrido[4,3-b]-7-azaindole (46).** Polyphosphoric acid (60 g) was added to **45** (7.69 g, 27.5 mmol) and the mixture stirred gently at 150 °C for 24 h. The mixture was cooled to RT, and ice (50 g) was added to break up the gum. The reaction mixture was made basified with 2 M NaOH (aq) and extracted with EtOAc ( $3 \times 300$  mL). The combined organic extracts were treated with brine (90 mL), dried ( $Na_2SO_4$ ), concentrated in vacuo, and adsorbed onto silica for purification by flash column chromatography (0–10% MeOH/ $CH_2Cl_2$ ). The mustard colored solid obtained (3.80 g) was triturated with a small volume of  $CH_2Cl_2$ , filtered, and dried to furnish the desired compound as a sand colored solid **57** (3.00 g, 42% yield). LCMS (+ve ESI):  $t_R = 0.97$  min, 264 ( $M + H$ )<sup>+</sup>.  $^1H$  NMR (400 MHz, DMSO)  $\delta$  2.80 (m, 4H), 3.57 (s, 2H), 3.73 (s, 2H), 6.94 (dd,  $J = 7.8, 4.7$  Hz, 1H), 7.21–7.42 (m, 5H), 7.67 (dd,  $J = 7.8, 1.2$  Hz, 1H), 8.07 (dd,  $J = 4.7, 1.5$  Hz, 1H), 11.32 (s, 1H).

**2,3,4,5-Tetrahydro-1-benzylpyrido[4,3-b]-7-azaindole (39a).** **46** (2.90 g, 11.0 mmol),  $NH_4CO_2H$ (s) (2.78 g, 44.0 mmol), and 20% PdOH on carbon (290 mg) were suspended in EtOH (200 mL) and stirred under reflux. After 1 h, more  $NH_4CO_2H$ (s) (695 mg, 11.0 mmol) was added and refluxing continued for 1 h. The catalyst was filtered off through Celite and washed with a small volume of  $CH_2Cl_2$ , and the combined filtrate was concentrated in vacuo and dried under vacuum to furnish the desired compound as off-white solid **39a** (1.90 g, 100% yield).  $^1H$  NMR (400 MHz, DMSO)  $\delta$  2.46–2.55 (m, 2H), 2.67 (t,  $J = 5.6$  Hz, 2H), 3.02 (t,  $J = 5.6$  Hz, 2H), 3.83 (s, 2H), 6.95 (dd,  $J = 7.7, 4.7$  Hz, 1H), 7.70 (dd,  $J = 7.7, 1.4$  Hz, 1H), 8.07 (dd,  $J = 4.7, 1.4$  Hz, 1H), 11.25 (s, 1H).

**(1R,2R)-N-(1-Cyanocyclopropyl)-2-[1,3,4,5-tetrahydro-1H-pyrido[4,3-b]-7-azaindol-2-yl)carbonyl]-cyclohexanecarboxamide (39).** **39a** (200 mg, 1.15 mmol) was utilized with **14c** (177 mg, 1.20 mmol) to furnish **39**, after purification, as an off-white solid (40.0 mg, 9% yield). HRMS (ES+) for  $C_{22}H_{26}O_2N_5$  ( $M^+ + H$ ): calcd 392.2081; found, 392.2084.  $^1H$  NMR (400 MHz, DMSO, 303 K)  $\delta$  0.72 (s, 1H), 0.69–0.80 (dd,  $J = 41.8, 7.8$  Hz, 0.5H), 0.93–1.30 (m, 1H), 1.15–1.45 (m, 6H), 1.62–1.85 (m, 4H), 2.67–2.75 (m, 0.5H), 2.78–2.84 (m, 0.5H), 2.95–3.05 (m, 1H), 3.69–3.82 (m, 0.5H), 3.84–3.94 (m, 1.5H), 4.52 (d,  $J = 15.8$  Hz, 0.5H), 4.65 (d,  $J = 15.8$  Hz, 0.5H), 4.75 (s, 1H), 7.02 (“ddd”,  $J = 16.6, 7.7, 4.8$  Hz, 1H), 7.83 (d,  $J = 7.6$  Hz, 0.5H), 7.93 (d,  $J = 7.6$  Hz, 0.5H), 8.13 (dd,  $J = 8.5, 4.4$  Hz, 1H), 8.71 (d,  $J = 3.7$  Hz, 1H), 11.44 (s, 1H).  $^1H$  NMR (500 MHz, DMSO, 373 K)  $\delta$  0.84–0.86 (m, 1H), 0.94 (d,  $J = 62.4$  Hz, 1H), 1.16–1.53 (m, 6H), 1.70–1.92 (m, 4H), 2.81 (m, 1H), 3.02 (td,  $J = 11.8, 3.5$  Hz, 1H), 3.83 (b, 1H), 3.89 (dt,  $J = 13.3, 5.6$  Hz, 1H), 4.66 (s, 2H), 6.98 (dd,  $J = 7.2, 4.7$  Hz, 1H), 7.80 (d,  $J = 7.2$  Hz, 1H), 8.12 (dd,  $J = 4.7, 1.5$  Hz, 1H), 8.27 (s, 1H), 11.04 (s, 1H).

**Assay for the Identification of Cat K Inhibitors.** QFRET Technology (quenched fluorescent resonance energy transfer) was used to measure the inhibition by test compounds of Cat K-mediated cleavage of the synthetic peptide Z-Phe-Arg-AMC. Compounds were screened at twelve concentrations (0.0003–10  $\mu M$ ), on two separate occasions, and the mean  $IC_{50}$  values reported.

A concentration of 0.5 nM [final] rhuman Cat K (prepared in-house) in phosphate buffer was added to a 384-well black microtiter plate containing investigative compounds. The enzyme and compound were preincubated at room temperature for 30 min before the addition of 50  $\mu M$  [final] Z-Phe-Arg-AMC synthetic substrate in sodium acetate/EDTA buffer at pH 5.5. The plates were covered and incubated for 1 h at room temperature and protected from light. Following the incubation, the reaction was stopped with 7.5% [final]

acetic acid. Relative fluorescence was measured using the Ultra plate reader at a wavelength of 360 nm excitation and 425 nm emission.

Data was corrected for background fluorescence (minimum controls without enzyme). This data was used to plot inhibition curves and calculate  $IC_{50}$  values by nonlinear regression using a variable slope, offset=zero model in Origin 7.5 analysis package. Reproducibility of data was assessed using a quality control statistical analysis package whereby internal variability of the assayed indicated a repeat testing ( $n = 3$ ) if  $pIC_{50}$  SD was  $>0.345$ .

**Assay for the Identification of Cat L Inhibitors.** In a similar manner using the same QFRET technology compounds were tested for inhibition of cathepsin L-mediated cleavage of a synthetic peptide Z-Phe-Arg-AMC (10  $\mu$ M final concentration) using 0.1 nM [final] r-human Cat L (prepared in-house). A potassium phosphate buffer was used to maintain pH at 6.4.

**Assay for the Identification of Cat S Inhibitors.** In a similar manner using the same QFRET technology, compounds were tested for inhibition of cathepsin S-mediated cleavage of a synthetic peptide Z-Val-Val-Arg-AMC (100  $\mu$ M final concentration) using 0.5 nM [final] r-human Cat S (prepared in-house). A potassium phosphate buffer was used to maintain pH at 6.4.

**Assay for the Identification of Cat B Inhibitors.** In a similar manner using the same QFRET technology, compounds were tested for inhibition of cathepsin B-mediated cleavage of a synthetic peptide Z-Arg-Arg-AMC (100  $\mu$ M final concentration) using 0.5 nM [final] r-human Cat B (prepared in-house). A potassium phosphate buffer was used to maintain pH at 6.4.

**Assay for the Identification of Cat K inhibitors in Dog.** In a similar manner using the same QFRET technology, compounds were tested for inhibition of cathepsin K-mediated cleavage of a synthetic peptide Z-Phe-Arg-AMC (15  $\mu$ M final concentration) using 0.5 nM [final] r-dog Cat K (prepared in-house). A sodium acetate buffer was used to maintain pH at 5.5.

**Dog Beagle Blood Bone Remodeling via ELISA Detection of CTX-1.** All pharmacodynamic work was carried out on a small colony of 6 male dogs (Alderley Park Beagle), at the age of 12–14 months, weighing 14–17 kg. All studies were started at the same time of day to standardize results against the normal 24 h circadian rhythm. Dogs were typically dosed with test compound by gavage (po), and blood samples for both PK and PD analysis were taken at predetermined time points via the jugular vein. Formulation of test compounds was in 5% DMSO + 95% HPMC/Tween, in a typical dosing volume of 5 mL/kg. PD sampling (serum): blood samples were allowed to clot for a minimum of 1 h, at room temperature, prior to being spun at 2000 rpm for 15 min. The serum was then removed and placed into appropriate tubing and stored at  $-20$  °C until analysis, after which the samples were stored at  $-80$  °C. Bone resorption: samples were analyzed for CTX-1 using a Nordic Bioscience Serum CrossLaps ELISA kit (4CRL4000). ELISA was carried out according to protocol, while data were analyzed using Molecular Devices Softmax Pro software installed on a Molecular Devices Versamax tunable plate reader. PK sampling (whole blood): 200  $\mu$ L of whole blood was placed into the appropriate well of a 96-well plate, containing 200  $\mu$ L of distilled water. Analysis was by LC-MS against standard concentration curves for compound **1**, after protein precipitation with cold  $CH_3CN$  and centrifugation.

**Crystallography.** Diffraction data for compound **14** were collected at 100 K on a beamline PX at the Swiss Light Source (SLS, Villigen, Switzerland). The structure was solved by molecular replacement and refined to a final resolution of 2.33 Å and an *R*-factor of 25.0% using the Collaborative Computational Project, Number 4 CCP4 (<http://www.ccp4.ac.uk>) CCP4 and Coot (<http://www.yasbl.york.ac.uk/~emsley/cool>) software packages. This structure has been deposited in the RSB (home.rcsb.org) Protein Data Bank ([www.rcsb.org/pdb/home/home.do](http://www.rcsb.org/pdb/home/home.do)) with reference code 4DMY.

## ■ ASSOCIATED CONTENT

### ■ Supporting Information

Details of synthesis of final compounds and intermediates;  $^1H$  NMR for compounds **13**, **14**, and **39** at 373 K; rat and human hepatic metabolite identification for **14** and **34**, and rat in vivo urinalysis metabolite identification for **39**. Table of data: dog PK/PD [CTX-1] for **34**; baseline [CTX-1] levels over 48 h for comparison of the magnitude of effect; dose to man prediction calculations; crystallization coordinates for Cat K/34 cocomplex. This material is available free of charge via the Internet at <http://pubs.acs.org>.

## ■ AUTHOR INFORMATION

### Corresponding Author

\*Phone: +44 (0) 1625 517673. Fax: +44 (0) 1625 516667. E-mail: [al.dossetter@astrazeneca.com](mailto:al.dossetter@astrazeneca.com).

### Notes

The authors declare no competing financial interest.

## ■ ABBREVIATIONS USED

OA, osteoarthritis; OP, osteoporosis; MBD, metastatic bone disease; Cat K, cathepsin K; Cat S, cathepsin S; cat B, cathepsin B; Cat L, cathepsin L; HATU, *O*-(7-azabenzotriazol-1-yl)-*N,N,N,N*-tetramethyluronium hexafluorophosphate; PYBOP, benzotriazolylloxy-tris(pyrrolidino)phosphonium hexafluorophosphate; DIPEA, diisopropylethylamine; LLE, ligand lipophilicity efficiency; HLM, human liver microsomes; RLM, rat liver microsomes; CTX-1, C-telopeptide fragment of type 1 collagen; QFRET, quenched fluorescent resonance energy transfer technology; CCP4, collaborative computational project, number 4

## ■ REFERENCES

- (1) Hunter, D. J.; Felson, D. T. Osteoarthritis. *BMJ [Br. Med. J.]* **2006**, *332*, 639–642.
- (2) Lawrence, R. C.; Felson, D. T.; Helmick, C. G.; Arnold, L. M.; Choi, H.; Deyo, R. A.; Gabriel, S.; Hirsch, R.; Hochberg, M. C.; Hunder, G. G.; Jordan, J. M.; Katz, J. N.; Kremers, H. M.; Wolfe, F. National Arthritis Data Workgroup Estimates of the prevalence of arthritis and other rheumatic conditions in the United States. Part II. *Arthritis Rheum.* **2008**, *58*, 26–35.
- (3) WHO Disease and Injury country estimates [http://www.who.int/healthinfo/global\\_burden\\_disease/estimates\\_country/en/index.html](http://www.who.int/healthinfo/global_burden_disease/estimates_country/en/index.html).
- (4) Felson, D. T.; Chaisson, C. E.; Hill, C. L.; Totterman, S. M.; Gale, M. E.; Skinner, K. M.; Kazis, L.; Gale, D. R. The association of bone marrow lesions with pain in knee osteoarthritis. *Ann. Intern. Med.* **2001**, *134*, 541–549.
- (5) Alzahrani, K.; Gandhi, R.; Debeer, J.; Petrucci, D.; Mahomed, N. Prevalence of clinically significant improvement following total knee replacement. *J. Rheumatol.* **2011**, *38*, 753–759.
- (6) Teitelbaum, S. L. Bone resorption by osteoclasts. *Science (Washington, D. C.)* **2000**, *289*, 1504–1508.
- (7) Gowen, M.; Lazner, F.; Dodds, R.; Kapadia, R.; Feild, J.; Tavaría, M.; Bertonecello, I.; Drake, F.; Zavarselk, S.; Tellis, I.; Hertzog, P.; Debouck, C.; Kola, I. Cathepsin K knockout mice develop osteopetrosis due to a deficit in matrix degradation but not demineralization. *J. Bone Miner. Res.* **1999**, *14*, 1654–1663.
- (8) Gupta, S.; Singh, R. K.; Dastidar, S.; Ray, A. Cysteine cathepsin S as an immunomodulatory target: present and future trends. *Expert Opin. Ther. Targets* **2008**, *12*, 291–299.
- (9) Stoch, S. A.; Wagner, J. A. Cathepsin K inhibitors: a novel target for osteoporosis therapy. *Clin. Pharmacol. Ther.* **2008**, *83*, 172–176.

- (10) Yasuda, Y.; Kaleta, J.; Broemme, D. The role of cathepsins in osteoporosis and arthritis: rationale for the design of new therapeutics. *Adv. Drug Delivery Rev.* **2005**, *57*, 973–993.
- (11) Yang, M.; Sun, J.; Zhang, T.; Liu, J.; Zhang, J.; Shi, M. A.; Darakhshan, F.; Guerre-Millo, M.; Clement, K.; Gelb, B. D.; Dolgiov, G.; Shi, G. Deficiency and Inhibition of Cathepsin K Reduce Body Weight Gain and Increase Glucose Metabolism in Mice. *Arterioscler., Thromb., Vasc. Biol.* **2008**, *28*, 2202–2208.
- (12) Vasiljeva, O.; Reinheckel, T.; Peters, C.; Turk, D.; Turk, V.; Turk, B. Emerging roles of cysteine cathepsins in disease and their potential as drug targets. *Curr. Pharm. Des.* **2007**, *13*, 387–403.
- (13) Gauthier, J. Y.; Chauret, N.; Cromlish, W.; Desmarais, S.; Duong, L. T.; Falguyret, J.; Kimmel, D. B.; Lamontagne, S.; Leger, S.; LeRiche, T.; Li, C. S.; Masse, F.; McKay, D. J.; Nicoll-Griffith, D. A.; Oballa, R. M.; Palmer, J. T.; Percival, M. D.; Riendeau, D.; Robichaud, J.; Rodan, G. A.; Rodan, S. B.; Seto, C.; Therien, M.; Truong, V.; Venuti, M. C.; Wesolowski, G.; Young, R. N.; Zamboni, R.; Black, W. C. The discovery of odanacatib (MK-0822), a selective inhibitor of cathepsin K. *Bioorg. Med. Chem. Lett.* **2008**, *18*, 923–928.
- (14) Stoch, S. A.; Zajic, S.; Stone, J.; Miller, D. L.; Van, D., K.; Gutierrez, M. J.; De, D., M.; Liu, L.; Liu, Q.; Scott, B. B.; Panebianco, D.; Jin, B.; Duong, L. T.; Gottesdiener, K.; Wagner, J. A. Effect of the Cathepsin K Inhibitor Odanacatib on Bone Resorption Biomarkers in Healthy Postmenopausal Women: Two Double-Blind, Randomized, Placebo-Controlled Phase I Studies. *Clin. Pharmacol. Ther. (N. Y., NY, U. S.)* **2009**, *86*, 175–182.
- (15) Eisman, J. A.; Bone, H. G.; Hosking, D. J.; McClung, M. R.; Reid, I. R.; Rizzoli, R.; Resch, H.; Verbruggen, N.; Hustad, C. M.; Da, S. C.; Petrovic, R.; Santora, A. C.; Ince, B. A.; Lombardi, A. Odanacatib in the treatment of postmenopausal women with low bone mineral density: three-year continued therapy and resolution of effect. *J. Bone Miner. Res.* **2011**, *26*, 242–251.
- (16) Yamashita, D. S.; Marquis, R. W.; Xie, R.; Nidamarthy, S. D.; Oh, H.; Jeong, J. U.; Erhard, K. F.; Ward, K. W.; Roethke, T. J.; Smith, B. R.; Cheng, H.; Geng, X.; Lin, F.; Offen, P. H.; Wang, B.; Nevins, N.; Head, M. S.; Haltiwanger, R. C.; Narducci, S.; Amy, A.; Liable-Sands, L. M.; Zhao, B.; Smith, W. W.; Janson, C. A.; Gao, E.; Tomaszek, T.; McQueney, M.; James, I. E.; Gress, C. J.; Zembryki, D. L.; Lark, M. W.; Veber, D. F. Structure–Activity Relationships of 5-, 6-, and 7-Methyl-Substituted Azepan-3-one Cathepsin K Inhibitors. *J. Med. Chem.* **2006**, *49*, 1597–1612.
- (17) Kumar, S.; Dare, L.; Vasko-Moser, J. A.; James, I. E.; Blake, S. M.; Rickard, D. J.; Hwang, S.; Tomaszek, T.; Yamashita, D. S.; Marquis, R. W.; Oh, H.; Jeong, J. U.; Veber, D. F.; Gowen, M.; Lark, M. W.; Stroup, G. A highly potent inhibitor of cathepsin K (relacatib) reduces biomarkers of bone resorption both in vitro and in an acute model of elevated bone turnover in vivo in monkeys. *Bone (San Diego, CA, U. S.)* **2007**, *40*, 122–131.
- (18) Bailey, A.; Pairaudeau, G.; Patel, A.; Thom, S. WO2004000825A1, 2003.
- (19) Black, W. C.; Percival, M. D. The consequences of lysosomotropism on the design of selective cathepsin K inhibitors. *ChemBioChem* **2006**, *7*, 1525–1535.
- (20) Falguyret, J.; Desmarais, S.; Oballa, R.; Black, W. C.; Cromlish, W.; Khougaz, K.; Lamontagne, S.; Masse, F.; Riendeau, D.; Toulmond, S.; Percival, M. D. Lysosomotropism of Basic Cathepsin K Inhibitors Contributes to Increased Cellular Potencies against Off-Target Cathepsins and Reduced Functional Selectivity. *J. Med. Chem.* **2005**, *48*, 7535–7543.
- (21) Hann, M. M.; Leach, A. R.; Harper, G. Molecular Complexity and Its Impact on the Probability of Finding Leads for Drug Discovery. *J. Chem. Inf. Comput. Sci.* **2001**, *41*, 856–864.
- (22) Crane, S. N.; Black, W. C.; Palmer, J. T.; Davis, D. E.; Setti, E.; Robichaud, J.; Paquet, J.; Oballa, R. M.; Bayly, C. I.; McKay, D. J.; Somoza, J. R.; Chauret, N.; Seto, C.; Scheiget, J.; Wesolowski, G.; Masse, F.; Desmarais, S.; Ouellet, M.  $\beta$ -Substituted Cyclohexanecarboxamide: A Nonpeptidic Framework for the Design of Potent Inhibitors of Cathepsin K. *J. Med. Chem.* **2006**, *49*, 1066–1079.
- (23) Robichaud, J.; Bayly, C. I.; Black, W. C.; Desmarais, S.; Leger, S.; Masse, F.; McKay, D. J.; Oballa, R. M.; Paquet, J.; Percival, M. D.; Truchon, J.; Wesolowski, G.; Crane, S. N.  $\beta$ -Substituted cyclohexanecarboxamide cathepsin K inhibitors: Modification of the 1,2-disubstituted aromatic core. *Bioorg. Med. Chem. Lett.* **2007**, *17*, 3146–3151.
- (24) Berkessel, A.; Glaubitz, K.; Lex, J. Enantiomerically pure  $\beta$ -amino acids: a convenient access to both enantiomers of trans-2-aminocyclohexanecarboxylic acid. *Eur. J. Org. Chem.* **2002**, 2948–2952.
- (25) Harbert, C. A.; Plattner, J. J.; Welch, W. M.; Weissman, A.; Koe, B. K. Neuroleptic activity in 5-aryltetrahydro- $\gamma$ -carboline. *J. Med. Chem.* **1980**, *23*, 635–643.
- (26) Ram, S.; Spicer, L. D. Debenzylation of N-benzylamino derivatives by catalytic transfer hydrogenation with ammonium formate. *Synth. Commun.* **1987**, *17*, 415–418.
- (27) Waring, M. J. Lipophilicity in drug discovery. *Expert Opin. Drug Discovery* **2010**, *5*, 235–248.
- (28) Andersson, S.; Armstrong, A.; Bjoere, A.; Bowker, S.; Chapman, S.; Davies, R.; Donald, C.; Egner, B.; Elebring, T.; Holmqvist, S.; Inghardt, T.; Johannesson, P.; Johansson, M.; Johnstone, C.; Kemmitt, P.; Kihlberg, J.; Korsgren, P.; Lemurell, M.; Moore, J.; Pettersson, J. A.; Pointon, H.; Ponten, F.; Schofield, P.; Selmi, N.; Whittamore, P. Making medicinal chemistry more effective-application of Lean Sigma to improve processes, speed and quality. *Drug Discovery Today* **2009**, *14*, 598–604.
- (29) Teague, S. J.; Davis, A. M.; Leeson, P. D.; Oprea, T. The design of leadlike combinatorial libraries. *Angew. Chem., Int. Ed.* **1999**, *38*, 3743–3748.
- (30) Oprea, T. I.; Davis, A. M.; Teague, S. J.; Leeson, P. D. Is There a Difference between Leads and Drugs? A Historical Perspective. *J. Chem. Inf. Comput. Sci.* **2001**, *41*, 1308–1315.
- (31) Williams, J. W.; Morrison, J. F. The kinetics of reversible tight-binding inhibition. *Methods Enzymol.* **1979**, *63*, 437–467.
- (32) Li, C. S.; Deschenes, D.; Desmarais, S.; Falguyret, J.; Gauthier, J. Y.; Kimmel, D. B.; Leger, S.; Masse, F.; McGrath, M. E.; McKay, D. J.; Percival, M. D.; Riendeau, D.; Rodan, S. B.; Therien, M.; Truong, V.; Wesolowski, G.; Zamboni, R.; Black, W. C. Identification of a potent and selective non-basic cathepsin K inhibitor. *Bioorg. Med. Chem. Lett.* **2006**, *16*, 1985–1989.
- (33) Johnson, T. W.; Dress, K. R.; Edwards, M. Using the Golden Triangle to optimize clearance and oral absorption. *Bioorg. Med. Chem. Lett.* **2009**, *19*, 5560–5564.
- (34) Leach, A. G.; Jones, H. D.; Cosgrove, D. A.; Kenny, P. W.; Ruston, L.; MacFaul, P.; Wood, J. M.; Colclough, N.; Law, B. Matched Molecular Pairs as a Guide in the Optimization of Pharmaceutical Properties; a Study of Aqueous Solubility, Plasma Protein Binding and Oral Exposure. *J. Med. Chem.* **2006**, *49*, 6672–6682.
- (35) Dossetter, A. G. A statistical analysis of in vitro human microsomal metabolic stability of small phenyl group substituents, leading to improved design sets for parallel SAR exploration of a chemical series. *Bioorg. Med. Chem.* **2010**, *18*, 4405–4414.
- (36) Lewis, M. L.; Cucurull-Sanchez, L. Structural pairwise comparisons of HLM stability of phenyl derivatives: Introduction of the Pfizer metabolism index (PMI) and metabolism-lipophilicity efficiency (MLE). *J. Comput.-Aided Mol. Des.* **2009**, *23*, 97–103.
- (37) Henderson, J. D.; Olson, R. D.; Ravis, W. R. Pharmacokinetic calculator program for generation of initial parameter estimates from a three-compartment infusion model. *J. Pharmacol. Methods* **1985**, *14*, 13–24.
- (38) McGinnity, D. F.; Collington, J.; Austin, R. P.; Riley, R. J. Evaluation of Human Pharmacokinetics, Therapeutic Dose and Exposure Predictions Using Marketed Oral Drugs. *Curr. Drug Metab.* **2007**, *8*, 463–479.
- (39) Sadick, M.; Attenberger, U.; Kraenzlin, B.; Kayed, H.; Schoenberg, S. O.; Gretz, N.; Schock-Kusch, D. Two non-invasive GFR-estimation methods in rat models of polycystic kidney disease: 3.0 T dynamic contrast-enhanced MRI and optical imaging. *Nephrol., Dial., Transplant.* **2011**, *26*, 3101–3108.

(40) Rowland, M.; Tozer, T. N. In *Clinical Pharmacokinetics; Concepts and Application*; 3rd ed., Chapter 11, p 171.

(41) Kuhn, B.; Mohr, P.; Stahl, M. Intramolecular Hydrogen Bonding in Medicinal Chemistry. *J. Med. Chem.* **2010**, *53*, 2601–2611.

(42) Ashwood, V. A.; Field, M. J.; Horwell, D. C.; Julien-Larose, C.; Lewthwaite, R. A.; McCleary, S.; Pritchard, M. C.; Raphy, J.; Singh, L. Utilization of an Intramolecular Hydrogen Bond To Increase the CNS Penetration of an NK1 Receptor Antagonist. *J. Med. Chem.* **2001**, *44*, 2276–2285.

(43) Sasaki, S.; Cho, N.; Nara, Y.; Harada, M.; Endo, S.; Suzuki, N.; Furuya, S.; Fujino, M. Discovery of a Thieno[2,3-*d*]pyrimidine-2,4-dione Bearing a *p*-Methoxyureidophenyl Moiety at the 6-Position: A Highly Potent and Orally Bioavailable Nonpeptide Antagonist for the Human Luteinizing Hormone-Releasing Hormone Receptor. *J. Med. Chem.* **2003**, *46*, 113–124.

(44) Rezaei, T.; Bock, J. E.; Zhou, M. V.; Kalyanaraman, C.; Lokey, R. S.; Jacobson, M. P. Conformational Flexibility, Internal Hydrogen Bonding, and Passive Membrane Permeability: Successful in Silico Prediction of the Relative Permeabilities of Cyclic Peptides. *J. Am. Chem. Soc.* **2006**, *128*, 14073–14080.

(45) Garnero, P.; Ferreras, M.; Karsdal, M.; Nicamhlaibh, R.; Risteli, J.; Borel, O.; Qvist, P.; Delmas, P. D.; Foged, N. T.; Delaisse, J. M. The type I collagen fragments ICTP and CTX reveal distinct enzymatic pathways of bone collagen degradation. *J. Bone Miner. Res.* **2003**, *18*, 859–867.

(46) Herrmann, M.; Seibel, M. The amino- and carboxyterminal cross-linked telopeptides of collagen type I, NTX-I and CTX-I: A comparative review. *Clin. Chim. Acta* **2008**, *393*, 57–75.

(47) Okuno, S.; Inaba, M.; Kitatani, K.; Ishimura, E.; Yamakawa, T.; Nishizawa, Y. Serum levels of C-terminal telopeptide of type I collagen: A useful new marker of cortical bone loss in hemodialysis patients. *Osteoporosis Int.* **2005**, *16*, 501–509.